Nuclear Instruments and Methods in Physics Research B 389–390 (2016) 23–27

Contents lists available at ScienceDirect

Nuclear Instruments and Methods in Physics Research B

journal homepage: www.elsevier.com/locate/nimb

Annealing bounds to prevent further Charge Transfer Inefficiency increase of the *Chandra* X-ray CCDs

Corentin Monmeyran [a,*], Neil S. Patel [a], Mark W. Bautz [b], Catherine E. Grant [b], Gregory Y. Prigozhin [b], Anuradha Agarwal [c], Lionel C. Kimerling [a,c]

[a] Department of Materials Science and Engineering, Massachusetts Institute of Technology, 77 Massachusetts Avenue, Cambridge, MA 02139, USA
[b] Kavli Institute for Astrophysics and Space Research, Massachusetts Institute of Technology, 77 Massachusetts Avenue, Cambridge, MA 02139, USA
[c] Microphotonics Center, Massachusetts Institute of Technology, 77 Massachusetts Avenue, Cambridge, MA 02139, USA

ARTICLE INFO

Article history:
Received 14 September 2016
Received in revised form 13 November 2016
Accepted 14 November 2016
Available online 22 November 2016

Keywords:
Irradiation
Point defect
Chandra
Charge Transfer Inefficiency
CCD
Proton
Annealing
Defect reaction
Interstitial
Carbon

ABSTRACT

After the front-illuminated CCDs on board the X-ray telescope *Chandra* were damaged by radiation after launch, it was decided to anneal them in an effort to remove the defects introduced by the irradiation. The annealing led to an unexpected increase of the Charge Transfer Inefficiency (CTI). The performance degradation is attributed to point defect interactions in the devices. Specifically, the annealing at 30 °C activated the diffusion of the main interstitial defect in the device, the carbon interstitial, which led to its association with a substitutional impurity, ultimately resulting in a stable and electrically active defect state. Because the formation reaction of this carbon interstitial and substitutional impurity associate is diffusion limited, we recommend a higher upper bound for the annealing temperature and duration of any future CCD anneals, that of −50 °C for one day or −60 °C for a week, to prevent further CTI increase.

1. Introduction

After the launch of the *Chandra* X-ray telescope in July 1999, its silicon CCDs were damaged by irradiation, causing increased Charge Transfer Inefficiency (CTI), from $< 10^{-6}$ to 2×10^{-4} (at −100 °C). In an effort to mitigate this damage, the CCDs were annealed to +30 °C for a few hours (the operating temperature being −100 °C). This operation resulted in a further 35% increase of the CTI. This degradation of performance following an anneal was referred to as "reverse annealing" in previous articles [1–3]. Now, more than 17 years later, another annealing of the device may occur as a side-effect of contemplated efforts to remove molecular contamination that has gradually accumulated on the optical blocking filters suspended just above the detectors. The filters are in reasonably good thermal contact with the detectors, and it is expected that warming the filters to remove contamination would also warm the detectors. Since the initial annealing, the CCD detectors have been exposed to additional radiation and hence have accumulated new defects which could result in another increase of the CTI if the detector temperature rises sufficiently. The goals of the work reported here are therefore: (i) to critically examine the hypothesis that the mechanism causing the "reverse annealing" is the association of the carbon-interstitial with substitutional impurities, resulting in electrically active defect states in the bandgap of the material; and (ii) to recommend an appropriate upper bound for the duration and temperature of future CCD anneals.

2. Review of the proposed mechanism

The Advanced X-ray Imaging Spectrometer (ACIS) instrument on the *Chandra* X-ray Observatory [4,5] contains buried channel silicon CCDs of two kinds: front illuminated and back illuminated, of which only the former were significantly damaged by exposure to radiation. The characteristics of the CCDs are described in detail elsewhere [6] and can be summarized as follows. The devices were

* Corresponding author.
E-mail addresses: comonmey@mit.edu (C. Monmeyran), neilp@mit.edu (N.S. Patel), mwb@space.mit.edu (M.W. Bautz), cgrant@space.mit.edu (C.E. Grant), gyp@space.mit.edu (G.Y. Prigozhin), anu@mit.edu (A. Agarwal), lckim@mit.edu (L.C. Kimerling).

http://dx.doi.org/10.1016/j.nimb.2016.11.020
0168-583X/

fabricated on 100-mm p-type float zone silicon wafers of resistivity of 7000 Ω·cm and therefore the background electrically active impurity concentration is deduced to be lower than 3×10^{12} cm^{-3}. This results in a depletion width of 50–70 μm. In addition to eventual electrically active impurities, high purity float-zone silicon contains carbon and oxygen at a 10^{15-16} cm^{-3} level. The CCDs have a buried channel which is obtained by an implantation of phosphorus through an oxide layer with an energy of 200 keV. After the various other processing steps and related annealings are performed, the phosphorus profile is a few hundreds of nanometers deep. In addition, the pixels have a trough, a 2 μm wide enhancement in the buried channel doping that makes the device more radiation hard [7–9]. The concentration of phosphorus in the buried channel and in the trough, where charges are collected and transfer after a light absorption event, is in the range of 10^{16} cm^{-3}. Therefore, in our analysis, we consider defects comprising vacancies, interstitials and their associates with carbon, oxygen and phosphorus.

Very detailed investigations [4,5,10] concluded that low energy protons ("soft" protons, with a kinetic energy in the hundreds of keV) were responsible for the damage during first few weeks of the flight, when detectors became exposed to soft protons during the passages through the radiation belts. Once the cause of the damage was identified, CCDs were moved out of the telescope focal position into the protected area during each radiation belt passage. That dramatically reduced the rate of damage accumulation (to ~2% a year) because population of soft protons is negligible outside the radiation belts. This is compatible with penetration depth of these particles. SRIM [11] was used to determine the ion range, straggle and primary defects (vacancies and interstitials, for both ionic and nuclear stopping regimes) generated in silicon by irradiation of protons of different energies, as shown in Table 1. 100 keV protons have an implantation depth of 860 nm in silicon, which is comparable to the depth of the buried channel of the CCDs, while protons of energies higher than 1 MeV will create most of their damage farther inside the bulk of the wafer and should therefore not alter the device performance as significantly. Protons of energies higher than 10 MeV can damage the front- and back-illuminated CCDs equally, but the latter were shown not to be affected by the initial radiation damage or, consequently, by the reverse annealing. In addition, the frame store section, which is shielded by 2.54 mm of gold coated aluminum, was not damaged. This is consistent with low energy proton damage, which cannot penetrate this metal shielding. All these considerations confirm that low energy protons are the most likely to have introduced defects that were involved in reverse annealing. This was confirmed by 100 keV proton irradiation experiments performed on the ground with similar CCD devices [2] which yielded CTI changes similar to observations on the annealed *Chandra* CCDs.

Irradiation damage creates Frenkel pairs, each pair consisting of one interstitial and one vacancy. The pair can split, leaving behind mono-vacancies and self-interstitials. Fig. 1 is a schematic of the transformation, as a function of the temperature, of the various defects observed in float-zone phosphorus-implanted silicon.

The mobility of defects at temperatures of interest can explain annealing-induced increase in CTI. At −100 °C, the operational temperature of the ACIS detectors in 1999, the mono-vacancies and self-interstitials created are mobile and will diffuse in the material until they form more energetically favorable complexes with impurities, such as oxygen, phosphorus and carbon. The resulting vacancy complexes (O-V, P-V and V-V) are present at −100 °C and stable up to 300 °C, and therefore not affected by annealing at +30 °C. The concentration of vacancy defects should therefore remain unaffected by the annealing. They contribute equally to the CTI before and after annealing and are not responsible for the additional performance degradation. In contrast, the carbon interstitial (C_I, the defect that forms from the association of the self-interstitial and a carbon atom) has a high mobility at the anneal temperature of +30 °C. For comparison, the ratio of diffusivity of the donor-vacancy pair and the carbon interstitial at +30 °C is 2×10^{-4}, as shown in Eq. (1) [13,14].

$$\frac{D_{P-V}}{D_{CI}} = \frac{9.7 \times 10^{-4} \exp\left(-\frac{0.93}{kT}\right)}{0.44 \exp\left(-\frac{0.87}{kT}\right)} = 2 \times 10^{-4} \quad (1)$$

In addition, vacancy-impurity complexes do not react with other impurities as much as the carbon interstitial, which, once mobile, will diffuse until it forms the more stable C_I-X_S complexes (with X_S a substitutional impurity, which in the case of the *Chandra* CCDs, is either phosphorus, oxygen or carbon) [15,16]. When the carbon interstitial diffuses, the probability that it forms a complex with an impurity X_S is proportional to the product of the X_S concentration and the reaction capture cross-section. In the buried channel, the active area, the highest concentration impurity is phosphorus (peak concentration of 3×10^{16} cm^{-3} whereas an upper bound for carbon and oxygen is 5×10^{15} cm^{-3}). Moreover, the capture cross-section of the formation of a phosphorus complex is two to twelve times higher than for an oxygen or carbon complex [16]. Therefore, the carbon interstitial will form more complexes with phosphorus than with other impurities.

We can conclude that the carbon interstitial (C_I) travels relatively rapidly at the annealing temperature to associate with a substitutional atom (X_S), forming a (C_I-X_S) complex, whose defect state has a different energy. In the case of the *Chandra* CCDs, the increase in CTI can be explained by the relative position of the defect states in the bandgap with respect to the Fermi energy, as is summarized in Fig. 2. We can calculate the quasi-Fermi level in the detector by approximating the number of injected carriers due to X-ray excitation. A typical charge packet in the on-board CCD contains 100–2500 electrons. In the following calculation, we will use the number of electrons in a packet generated by the X-ray calibration source of the telescope at −100 °C: 1600 electrons. This will determine the carrier concentration inside the device and hence the Fermi level position and the behavior of the different traps present in the device. To estimate the charge profile distribution, we have used profiles simulated in CCDs with a similar architecture [17]. The devices in the said simulation do not have a trough, but this is the only main difference with the *Chandra* CCDs. The presence of a trough is equivalent to having the width of a pixel shrunk to the size of the trough. The simulated profiles are done in a 27 μm × 27 μm pixel, and the *Chandra* trough are 2 μm. This

Table 1
Ion range, straggle and primary defects (vacancies and interstitials, for both ionic and nuclear stopping regimes) generated in silicon by irradiation of protons of different energies (calculated by SRIM).

Proton energy	Ion range (um)	Straggle (nm)	Number of primary defects generated in the ionic stopping regime (cm^{-3}/(ion·cm^{-2}))	Number of primary defects generated in the nuclear stopping regime (cm^{-3}/(ion·cm^{-2}))
100 keV	0.86	82	4×10^4	1.5×10^5
1 MeV	16.6	514	4×10^3	5×10^4
10 MeV	714	14×10^3	3×10^2	5×10^3

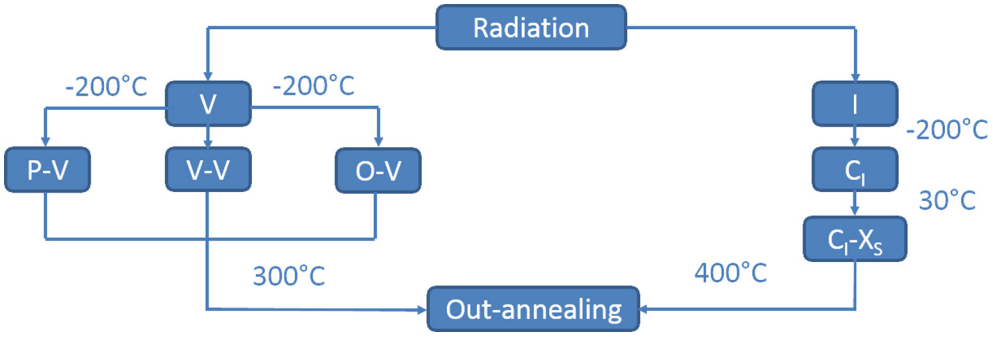

Fig. 1. Schematic of the point defect changes in n-type float zone silicon as a function of the temperature. The mono-vacancies and the self-interstitials form complexes with impurities at −200 °C. Then the vacancy associates are stable up to 300 °C, while the carbon interstitials will pair with a substitutional impurity at 30 °C until it out-anneals at 400 °C [12].

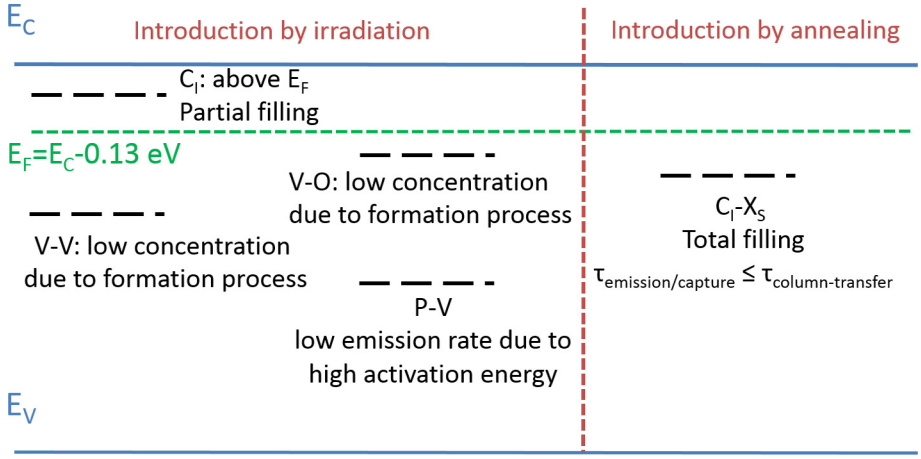

Fig. 2. Various defects present in the active region of the *Chandra* CCDs. The defects that contribute the most to the CTI are located below and close to the Fermi energy, which explains why the conversion of C_I into C_I-X_S increased the CTI.

means that a shrinking ratio of 13.5 is a good approximation: a 1600 electrons charge packet is equivalent to a 22,000 electrons packet in the simulated CCDs, which corresponds to a carrier concentration of 3×10^{15} cm^{-3} and a quasi-Fermi level 0.13 eV below the conduction band at −100 °C. Therefore, the defect state of the carbon interstitial (E_C −0.1 eV) is above the quasi-Fermi level and its occupation (Fermi factor) is f = 8%. It follows that its emission rate is much higher than its capture rate (Eq. (2), in which n, v, σ, N_C, E_F, E_T, E_C respectively denote the free carrier concentration, the thermal speed of the carrier, the capture cross-section of the defect, density of states of the conduction band, the (quasi)-Fermi energy, the deep-state level and the level of the conduction band). This means that most of the traps due to carbon interstitials are empty and only a fraction of them contribute to a loss of charge during the pixel-to-pixel charge transfer. This is not the case for the C_I-X_S created in the annealing process; these have deeper states than the quasi-Fermi level (for instance C_I-P_S has multiple metastable states, respectively 0.23, 0.26, 0.32 and 0.38 eV below the conduction band [18]). Even for the shallowest of the C_i-P_S for instance, the Fermi factor at −100 °C for a 1620 electron pulse is 0.998, an order of magnitude higher than for the donor level of the carbon interstitial. Consequently, even if the number of traps is the same before and after the reverse annealing, the effective number of traps contributing to the capture of electrons is much higher after the reverse annealing.

$$\frac{c_n}{e_n} = \frac{n v \sigma}{N_c v \sigma \exp\left(-\frac{E_c - E_T}{kT}\right)} = \exp\left(\frac{E_F - E_T}{kT}\right) \quad (2)$$

The vacancy-defects (P-V, O-V and V-V, which were detected in the *Chandra* CCDs using a variation of DLTS [10]) do affect the CTI, which is why the performance of the CCDs degraded after launch, even before the annealing. However, due to their position in the bandgap, these three defects have a different impact on the CTI. In n-type phosphorus-doped float zone silicon, which constitutes the buried channel, the defect with the highest concentration, is the phosphorus-vacancy pair [19]. It is deep in the bandgap (E_C −0.44 eV). Consequently, its emission rate is small: its characteristic time for emission is more than a second (to compare with the pixel-to-pixel transfer rate, of 40 μs). As a result, the P-V states are filled with electrons during radiation exposure, and do not re-emit or capture additional charges during their transfer from one column to the other (Indeed, the CCD operating temperature was chosen in part to minimize the effect of radiation-induced P-V centers on the CTI and the dark current). On the other hand, the oxygen-vacancy (O-V) and the di-vacancy have defect states respectively 0.18 eV and 0.23 eV below the conduction band, and emission and capture rates fast enough (<μs) to interact with charges during the pixel-to-pixel transfers (40 μs). They therefore contribute to the Charge Transfer Inefficiency. In summary, most of the vacancy-defects in the buried channel are P-V centers, which have too low an emission rate to significantly affect the CTI. After irradiation and before annealing, the CTI is due to the C_I which are only partially active and the V-V and O-V complex that are present at smaller concentrations.

Only the C_I-X_S complexes are responsible for the increase of CTI due to the reverse annealing and their formation is

diffusion-limited. A crucial assumption of this hypothesis is the existence of a high concentration of sinks for the carbon interstitials. This assumption is validated by the on-ground CCD irradiation study reported by Grant et al. [2]. In these experiments, a soft proton (i.e. with a kinetic energy in the hundred of keV) irradiation could replicate the increase of CTI with doses of 10^8 protons cm^{-2} [2], which is equivalent to an introduction of $10^{13}\,cm^{-3}$ interstitials, consistently with the estimate from the Stopping and Range of Ions in Matter (SRIM) software (Table 1). Therefore, the carbon-interstitial concentration C_I ($\approx 10^{13}\,cm^{-3}$) is indeed dilute compared to the concentration ($10^{15-16}\,cm^{-3}$) of the substitutional C or P impurities, confirming that post-anneal CTI saturates due to the consumption of all the carbon interstitials and not due to the consumption of the substitutional impurities. Moreover, the CCDs have experienced a gradual defect build-up over their 17 years lifetime, because of the radiation background in space. This defect introduction (mostly O-V, P-V, V-V and C_I, as shown in Fig. 1) has resulted in an increase of the CTI of 2% per year. Consequently, there are both enough sinks and carbon interstitials in the material to fuel a significant reverse annealing, should the temperature be raised.

The formation of the general C_I-X_S complex is limited by the diffusion of the carbon interstitial, whose diffusivity is $D_{C1} = 0.44 \exp\left(\frac{-}{0.87\ eV} kT\right) cm^2\ S^{-1}$ [13]. Fig. 4 represents the distance travelled by diffusion by C_I (defined by Eq. (4)) as a function of annealing temperature for different annealing durations, as well as the typical distance between background impurities and the inter-atomic distance in a silicon crystal. Because for a diffusion-limited reaction in the limit where the concentration of C_I is small compared to the concentration of X_S, the formation of a C_I-X_S complex saturates when the diffusion length is of the same order of magnitude as that of the average distance between X_S atoms as shown in Fig. 3 and Eq. (3).

$$L_D \approx [X_s]^{-1/3} \tag{3}$$

this figure can be used to determine an upper limit for the annealing duration and temperature to prevent the diffusion to a sink of a certain concentration. It is consistent with the reverse annealing observed on the ground, during which the CTI increased during a few hours at +30 °C before saturating [2]. Indeed, for such an anneal, the diffusion length of the carbon interstitial corresponds to the distance between background impurities, as described by Eq. (3)

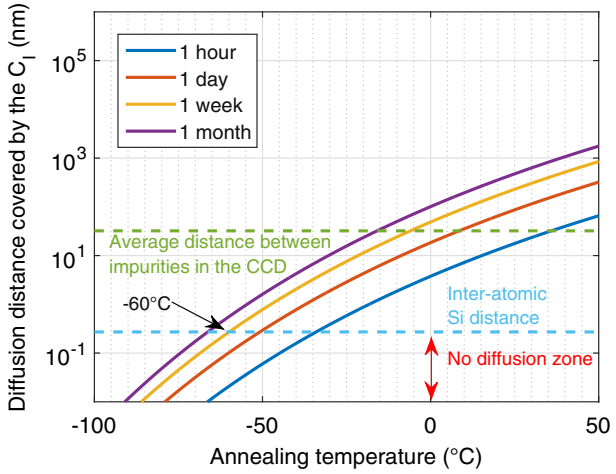

Fig. 4. Diffusion length of the carbon interstitial as a function of the annealing temperature, for various annealing durations. The average distance between impurities in the CCDs (calculated to correspond to a concentration of $3 \times 10^{16}\,cm^{-3}$, the maximal concentration of phosphorus in the buried channel. It is also an upper bound for the background concentration of carbon and oxygen) and the inter-atomic distance of silicon atoms are indicated.

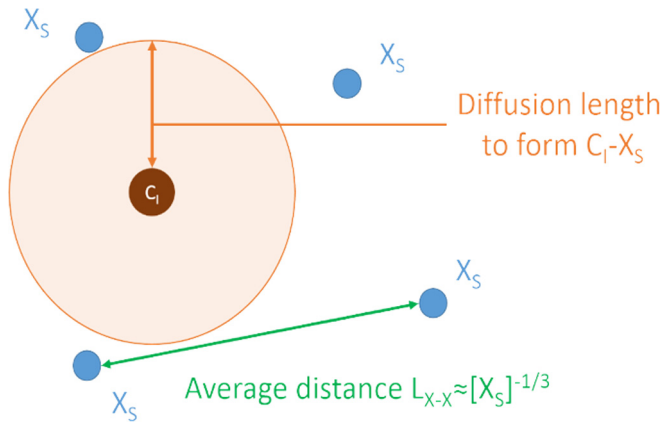

Fig. 3. Schematic of the average distance between impurities and the diffusion length of C_I. The formation C_I-X_S happens when the diffusion length is of the same order of magnitude as that of the average distance between X_S's.

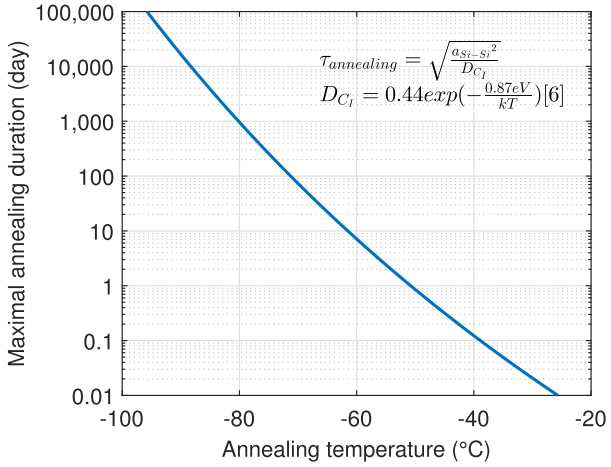

Fig. 5. Maximal annealing duration versus annealing temperature to avoid diffusion of the C_I and the formation of C_I-X_S. The diffusion is blocked for annealing durations and temperatures below the blue curve.

and (4). As the diffusion distance gets closer to the lattice parameter, this continuous model breaks down. The diffusion indeed becomes a discreet random walk, where the carbon-interstitial has a certain probability to hop from one site to another neighboring site. It means that the probability of even one jump of the C_I is low and that diffusion is effectively blocked. In order to prevent a further increase of CTI, the annealing parameters should hence be chosen to be in this "no-diffusion" regime. Fig. 5 shows the onset of this regime as a function of annealing temperature, for instance 1 week at −60 °C or one day at −50 °C.

$$L_D = \sqrt{D_{c1}\,\tau_{annealing}} \tag{4}$$

3. Conclusion

In the seventeen years since the *Chandra* launch, the CCDs have continued to be irradiated at a slow rate, with a CTI increase of roughly 2%/year. The additional CTI is a sign that new defects have been introduced in the CCDs, and that an anneal will result in further degradation of the CTI, similarly to what happened in 1999. The CTI increase was due to the diffusion limited reaction of carbon interstitial with impurities in the material, which resulted in the formation of more electrically active defects. To prevent such a "reverse annealing", the diffusion of the carbon interstitial needs to be

prevented, which can be done by not exceeding the following conditions: (i) a week long anneal at −60 °C or (ii) a one day anneal at −50 °C.

Acknowledgement

This work was funded by the Defense Threat Reduction Agency, grant number HDTRA1-13-1-0001.

Appendix A. Supplementary data

Supplementary data associated with this article can be found, in the online version, at http://dx.doi.org/10.1016/j.nimb.2016.11.020.

References

[1] M. Bautz, G. Prigozhin, S. Kissel, B. LaMarr, C. Grant, S. Brown, Anomalous annealing of a high-resistivity CCD irradiated at low temperature, IEEE Trans. Nucl. Sci. 52 (2) (2005) 519–526.
[2] C.E. Grant, B. LaMarr, G.Y. Prigozhin, S.E. Kissel, S.K. Brown, M.W. Bautz, Physics of reverse annealing in high-resistivity *Chandra* ACIS CCDs, Proc. SPIE 7021 (2008) 702119–702119–9.
[3] K. Kono, J.G. Sandland, K. Wada, L.C. Kimerling, Evaluation of irradiation-induced deep levels in Si, Proc. SPIE 4140 (2000) 267–273.
[4] G.P. Garmire, M.W. Bautz, P.G. Ford, J.A. Nousek, G.R. Ricker Jr, Advanced CCD imaging spectrometer (ACIS) instrument on the Chandra X-ray observatory, Proc. SPIE 4851 (2003) 28–44.
[5] M.C. Weisskopf, B. Brinkman, C. Canizares, G. Garmire, S. Murray, L.P.V. Speybroeck, An overview of the performance and scientific results from the Chandra X-Ray observatory, Publ. Astron. Soc. Pac. 114 (791) (2002) 1.
[6] B.E. Burke et al., Soft-X-ray CCD imagers for AXAF, IEEE Trans. Electron Devices 44 (10) (1997) 1633–1642.
[7] R.A. Bredthauer, J.H. Pinter, J.R. Janesick, L.B. Robinson, Notch and large-area CCD imagers, Proc. SPIE 1447 (1991) 310–315.
[8] W.F. Kosonocky, Charge-coupled device channel structure, US4667213 A, 19-May-1987.
[9] R.D. Nelson, Potential troughs for charge transfer devices, US4185292 A, 22-Jan-1980.
[10] G.Y. Prigozhin et al., Characterization of the radiation damage in the Chandra x-ray CCDs, Proc. SPIE 4140 (2000) 123–134.
[11] J.F. Ziegler, M.D. Ziegler, J.P. Biersack, SRIM–The stopping and range of ions in matter (2010), Nucl. Instrum. Methods Phys. Sect. B Beam Interact. Mater. At. 268 (11–12) (2010) 1818–1823.
[12] G.L. Miller, D.V. Lang, L.C. Kimerling, Capacitance transient spectroscopy, Annu. Rev. Mater. Sci. 7 (1) (1977) 377–448.
[13] A.K. Tipping, R.C. Newman, The diffusion coefficient of interstitial carbon in silicon, Semicond. Sci. Technol. 2 (5) (1987) 315.
[14] M. Yoshida, E. Arai, H. Nakamura, Y. Terunuma, Excess vacancy generation mechanism at phosphorus diffusion into silicon, J. Appl. Phys. 45 (4) (Apr. 1974) 1498–1506.
[15] L.F. Makarenko, M. Moll, F.P. Korshunov, S.B. Lastovski, Reactions of interstitial carbon with impurities in silicon particle detectors, J. Appl. Phys. 101 (11) (2007) 113537.
[16] L.C. Kimerling, M.T. Asom, J.L. Benton, P.J. Drevinsky, C.E. Caefer, Interstitial defect reactions in silicon, Mater. Sci. Forum 38 (1991) 141–150.
[17] T. Hardy, R. Murowinski, M.J. Deen, Charge transfer efficiency in proton damaged CCD's, IEEE Trans. Nucl. Sci. 45 (2) (1998) 154–163.
[18] E. Gurer, B. Benson, G. Watkins, Configurational metastability of carbon-phosphorus pair defects in silicon, in: G. Davies, G.G. Deleo, M. Stavola (Eds.), Proceedings of the 16th International Conference on Defects in Semiconductors, Pts 1–3, 83, Trans Tech Publications Ltd, Stafa-Zurich, 1992, pp. 339–344.
[19] G.D. Watkins, J.W. Corbett, Defects in irradiated silicon: electron paramagnetic resonance and electron-nuclear double resonance of the Si-E center, Phys. Rev. 134 (5A) (1964) A1359–A1377.